4th Intercontinental Geoinformation Days

igd.mersin.edu.tr

Comparison of the effect of different vegetation indices on land surface temperature values

Gulshan Mammadli*[1], Filiz Bektas Balcik[2]

[1]*Istanbul Technical University, Informatics Institute, Applied Informatics Department, Istanbul, Türkiye*
[2]*Istanbul Technical University, Civil Engineering Faculty, Geomatics Engineering Department, Istanbul, Türkiye*

Keywords
Remote sensing
Vegetation indices
Mono-window algorithm
NDVI threshold
Land cover map

Abstract

Land surface temperature (LST), which is a very important parameter in many fields such as ecology, hydrology and climate studies, can be monitored on a regional and global scale with satellite images. This study aimed to investigate the effects of different Vegetation indices (VI) on LST. The study focused on to generate LST maps over North-Rhine-Westphalia and Rhineland-Palatinate states of German using 23 August 2016 dated Landsat 8 OLI&TIRS data. Additionally, Sentinel-FCOVER data was used to examine the effect of VI on LST. The LST values were retrieved with Mono-window method, and Land Surface Emissivity (LSE) maps were calculated with $NDVI_{THM}$ method. Normalized Difference Vegetation Index (NDVI), Renormalized Difference Vegetation Index (RDVI), Soil Adjusted Vegetation Index (SAVI), Enhanced Vegetation Index (EVI) were selected for the study. Additionally, soil emissivity values were calculated from LUCAS (Land Use and Coverage Area frame Survey) and ASTER Spectral Libraries datasets. Finally, the accuracy of FVC (Fractional vegetation cover) and LST maps were evaluated. Although the best FVC result was achieved with RDVI, LST maps showed similar results for all selected vegetation indices. Thus, transects were extracted from the LST maps for different land cover categories and the results were compared to determine the differences.

1. Introduction

The Land Surface Temperature (LST) parameter, which refer to the temperature of the Earth's surface is one of the important factors in hydrology, ecology and global change studies. Thermal remote sensing technologies provide unique methods for collecting LST information on both a regional and global scale (Yu et al. 2014).

Land Surface Emissivity (LSE) parameter is very important to calculate LST from thermal band. Many different methods have been developed to calculate LSE from remotely sensed data. The NDVI threshold ($NDVI_{THM}$) method is one of the most widely used approaches to determine LSE (Sobrino et al. 2008; Sobrino and Raissouni 2000). This method is based on the NDVI index. There are many studies in the literature evaluating the effects of LSE on LST (Sekertekin and Bonafoni 2020a; Sekertekin and Bonafoni 2020b;). However, there are very few studies investigating the effect of the VI factor on LST. One of these studies was carried out by Neinavaz et al. (2020). In their study, the VARIgreen, WDRVI, TGDVI VIs in addition to NDVI index were evaluated using $NDVI_{THM}$ method. The result of the study showed that LSE is not the only factor to effect LST values. Therefore, LST_{WDRVI} and LST_{TGDVI} maps were had higher accuracy than LST_{NDVI} and $LST_{VARIgreen}$ maps.

The aim of our study was to investigate and compare the performance of selected VIs as NDVI, RDVI, SAVI and EVI on LST calculation according to land cover classes (Mammadli 2022).

2. Method

In this study, Germany's North Rhine Westphalia and Rhineland Palatinate states were chosen as the test area.

Within the scope of the study, the LST maps were retrieved from August 23, 2016 dated Landsat 8 OLI & TIRS data using the Mono-window (MW) method. To implement the MW algorithm, atmospheric parameters and emissivity values are required. To calculate atmospheric parameters, water vapor (ω) and near-surface temperature (T0) data were gathered from DWD

* **Corresponding Author**

*(mammadlig19@itu.edu.tr) ORCID ID 0000-0003-2063-9971
(bektasfi@itu.edu.tr) ORCID ID 0000-0003-3039-6846

Cite this study

Mammadli, G., & Balcik, F. B. (2022). Comparison of the effect of different vegetation indices on land surface temperature values. 4th Intercontinental Geoinformation Days (IGD), 28-31, Tabriz, Iran

(Germany weather station) meteorological stations. Additionally, two different Sentinel-2A products were used to evaluate the accuracy of the FVC and Land Cover (LC) maps.

Sentinel-FCOVER data were used to examine the FVC results were produced by using selected VIs. ASTER spectral library and LUCAS soil samples were used to calculate soil emissivity values in the NDVI threshold method.

2.1. Vegetation index calculation

NDVI, RDVI, SAVI and EVI vegetation indices were used to investigate the effects of spectral indices on LST. These VIs were integrated to the emissivity equation as input parameters. The original NDVI threshold method uses the NDVI index. The main reasons for choosing other indices were summarized below;

i) The SAVI index, unlike the NDVI index, helps to minimize the effects caused by soil reflection and provides a contribution to this index.

ii) The RDVI index provides improvement in background effects caused by geometry and ground.

iii) The EVI vegetation index optimizes vegetation signals by eliminating background reflection and saturation problems, as well as atmospheric pollution caused by dust and clouds.

Equations developed for VIs are given in Table 1.

Table 1. Vegetation indices equations

Index	Equation	Referance
NDVI	(B5-B4)/(B5+B4)	Rouse et al. (1973)
EVI	2.5*((B5-B4)/B5+B4-7.5*B2+1))	Jiang et al. (2008)
RDVI	$(B5-B4)/(B5+B4)^{1/2}$	Roujean and Breon (1995)
SAVI	1.5*((B5-B4)/B5+B4+0.5))	Huete (1988)

2.2. LST calculation

The MW algorithm was proposed by Qin et al. (2001) to calculate LST from Landsat TM data. The improved MW algorithm was used in this study to calculate LST values (Wang et al. 2015).

2.2.1. Land surface emissivity calculation

The LSE values integrated into the LST maps were calculated with the NDVI threshold method.

2.2.2. $NDVI_{THM}$ method

This method assumes that the satellite image pixels are composed of vegetation, soil or mixed pixels. An equation is proposed for each of these approaches. Soil, vegetation emissivity values and FVC map are required to use the equations. FVC maps were calculated from vegetation indices (Sobrino and Raissouni 2000). Vegetation emissivity value (0.99) was selected from the literature. The emissivity values of mixed pixels were estimated from FVC. Contrary to vegetation, soil emissivity values were calculated from the ASTER spectral library and LUCAS soil sample since soil have a high emissivity variation. LUCAS soil samples were used to determine the soil classes of the test area, and the ASTER spectral library were used to extract the soil reflectance. Multiple regression analysis was applied to the soil reflectance values to estimate the average soil emissivity and band coefficients (Li & Jiang 2018).

2.2.3. Mono-window method

In order to calculate the LST with the MW algorithm, first atmospheric transmission (τ) and effective mean atmospheric temperature (Ta) values were estimated from ω and T0. This data was collected by DWD Germany Weather Station. After τ and Ta values were calculated, Landsat 8 thermal band 10 first was converted to TOA radiance and then BT was calculated. The required data for this process were extracted from the metadata file of Landsat 8 OLI & TIRS.

2.3. Accuracy assessment

The accuracy assessment of the FVC and LST maps were performed by means of statistical parameters such as R^2 (Coefficient of determination), RMSE (Root Mean Square Error), MSE (Mean Squared Error), MAE (Mean Absolute Error) and Correlation.

2.4. Land cover map

In this study, in order to examine the spatial distribution of LST, five LC classes were determined and classified using the Maximum Likelihood method. The accuracy assessment of this map was performed using error matrix.

3. Results

The VI maps created from the Landsat 8 OLI & TIRS satellite image are shown in Fig 1.

3.1. Results of FVC maps

In the study, FVC maps were calculated by means of vegetation indices, soil and vegetation emissivity values, and accuracy was evaluated based on Sentinel-FCOVER data. FVC values ranged from 0 to 1. For case FVC=0; the soil emissivity value was calculated as 0.9695 in the study. According to the results of the FVC maps, RDVI has the highest accuracy (Table 2).

Table 2. FVC results for each index

Index	R2	RMSE	MSE
NDVI	0.60	0.285	0.081
EVI	0.68	0.248	0.062
RDVI	0.73	0.207	0.043
SAVI	0.70	0.215	0.046

3.2. Results of LC map

In the study, five main classes were determined and classified from the Landsat 8 OLI & TIRS image to evaluate the relationship of LST with LC classes (Fig. 2).

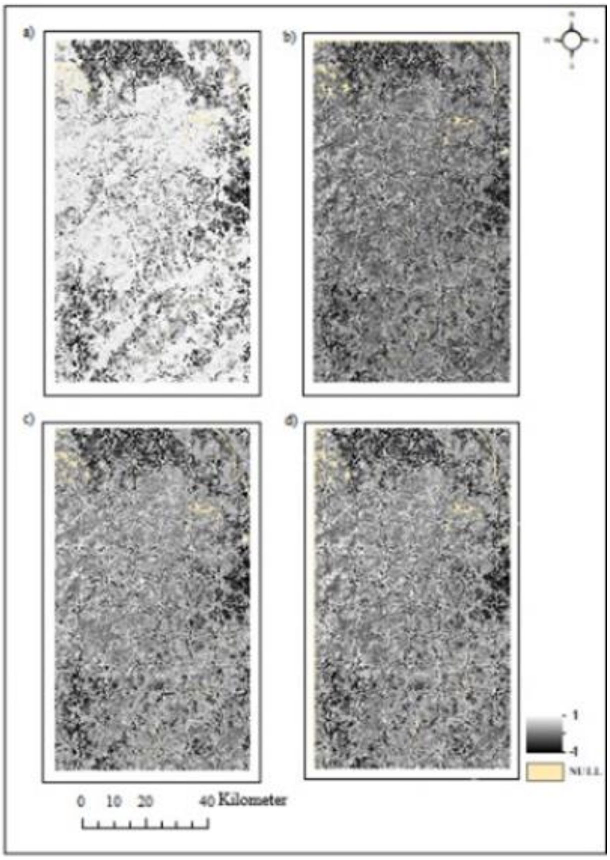

Figure 1. Vegetation index maps; a) forest & green areas b) agricultural areas, c) bareland d) artificial surfaces

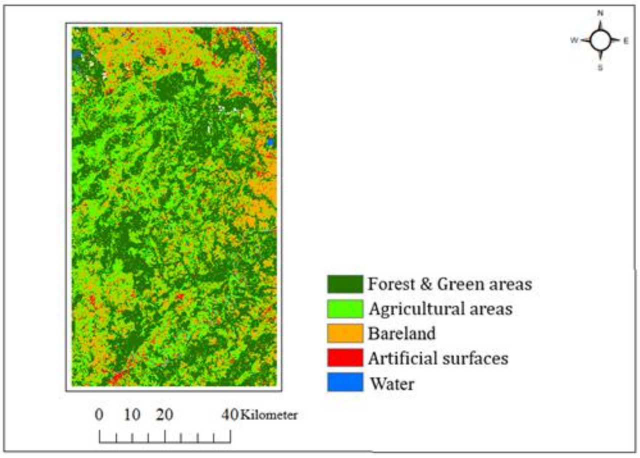

Figure 2. Land Cover map

According to the results of the LC map, the LST decreased with the increase of vegetation cover. The overall accuracy of the LC map is 0.89 based on error matrix and Kappa statistics is 0.85.

3.3. Result of LST

The accuracy assessment of the LST maps were carried out using 13 meteorological stations. R^2, RMSE, MAE, Correlation statistical parametres were calculated for each LST map. According to the statistical analysis results of the LST maps that were produced using selected vegetation indices, the LST values were relatively similar (Table 3).

Table 3. LST results for each selected index

Index	R^2	RMSE	MAE	Correlation
NDVI	0.588	1.882	1.331	0.767
EVI	0.585	1.931	1.379	0.765
RDVI	0.581	1.904	1.348	0.762
SAVI	0.581	1.904	1.348	0.762

Then transects were obtained and analysed from the images to reveal the existing differences between the LST values. These transects were extracted according to LC classes. First transects were created for forest & green areas, and agricultural areas (Fig 3.).

Figure 3. LST transects a) forest & green b) agricultural areas

The color scale in the graphs shows the temperature curves of the indices. Also transects for artificial surfaces and bareland were extracted from LST that calculated using selected VI (Fig. 4).

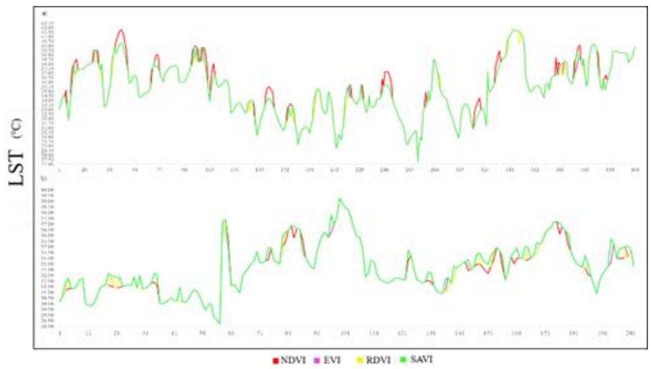

Figure 4. LST transects a) artificial surfaces b) bareland

According to these graphs, some pixel samples of LST_{NDVI} values were showed different results than the other three indices. The RDVI index and SAVI indices were showed very similar curves. The EVI index has relatively different values only in forest & green area classes.

4. Discussion

The results of the study showed that the effects of indices on the LST are quite low. In order to find out the reasons of this result, studies investigating the effects of LSE values calculated from VIs on LST were examined.

According to researches; The MW method is sensitive to parameters such as LSE, ω and Ta. Sensitivity analysis of the MW algorithm performed by Qin et al. (2001) and Wang et al. (2015) found that LST error dT was less sensitive to LSE compared to other parameters (ω, Ta). Additionally, LST error increase with the brightness temperature.

Jiang and Lin (2021), Sekertekin and Bonafoni (2020b), Windahl and Beurs (2016) have determined that the LST values for the winter and nighttime show more accurate results due to the decrease in the brightness temperature.

Neinavaz et al. (2020) suggested that specific factors of the study area, such as elevation or soil moisture, should also be included in the equation.

5. Conclusion

The temperature parameter has a significant effect on living and non-living things. These effects cause both positive and negative implication. Many studies focus on the negative aspects of these effects. Today, the sharp effects of the temperature increase cause environmental problems on a global scale. Continuous data is required to avoid from these effects. Remote sensing technologies is very effective to obtain the high temporal resolution data for large areas to quickly identify and solve the problems.

Within the scope of this study, the effect of different vegetation indices on LST calculation was investigated and evaluated. In the study, it was determined that the LST results were relatively similar and the effect of the indices on LST was quite low. Field studies could be carried out to support the results of this study. In addition, other factors affecting LST calculation should be investigated and evaluated in the study area. The emissivity effects of artificial surfaces are not addressed in this study.

Acknowledgement

We are grateful to the NextGEOSS project team, German Weather Service DWD, the European Soil Data Centre ESDAC and the ECOSTRESS Spectral Library for the data they have provided.

References

Huete, A. R. (1988), A Soil-adjusted vegetation index (SAVI), Remote Sensing of Environment, 25, 295-309.

Jiang, Z., Huete, A. R., Didan, K., & Miura, T. (2008). Development of a two-band enhanced vegetation index without a blue band. Remote Sensing of Environment, 112, 3833-3845.

Li, S., & Jiang, G. M. (2018). Land surface temperature retrieval from Landsat-8 data with the generalized split-window algorithm. IEEE Access, 6, 18149–18162, https://doi.org/10.1109/ACCESS.2018.2818741.

Mammadli, G. (2022). Farklı uzaktan algılama bitki indekslerinin Yer Yüzey Sıcaklığı hesabına etkisinin araştırılması. MS Thesis, Istanbul Technical University, Istanbul.

Neinavaz, E., Skidmore, A. K., & Darvishzadeh, R. (2020). Effects of prediction accuracy of the proportion of vegetation cover on land surface emissivity and temperature using the NDVI threshold method. International Journal of Applied Earth Observation and Geoinformation (JAG), 85, 1-13. [101984]. https://doi.org/10.1016/j.jag.2019.101984.

Qin, Z., Karnieli, A., & Berliner, P. (2001). A mono-window algorithm for retrieving land surface temperature from Landsat TM data and its application to the Israel-Egypt border region. International Journal of Remote Sensing, 22 (18), 3719–3746.

Rouse, J. W., Haas, R. H., Schell, J. A., Deering, D. W. (1973), Monitoring the vernal advancement and retrogradation of natural vegetation. Type II, Progress Report RSC 1978-1.

Roujean, J. L., & Breon, F. M. (1995). Estimating PAR absorbed by vegetation from bidirectional reflectance measurements. Remote Sensing of Environment, 51, Issue 3, https://doi.org/10.1016/0034-4257(94)00114-3.

Jiang, Y., & Lin, W. (2021). A Comparative analysis of retrieval algorithms of Land Surface Temperature from Landsat-8 Data: A case study of Shanghai, China. International Journal of Environmental Research and Public Health, 18, 5659. https://doi.org/10.3390/ijerph18115659.

Sobrino, J. A., & Raissouni, N. (2000) Toward remote sensing methods for Land Cover Dynamic Monitoring: application to Morocco. International Journal of Remote Sensing, 21, 353-366.

Sobrino, J. A., Jimenez-Munoz, J. C., Soria, G., Romaguera, M., Guanter, L., Moreno, J., Plaza, A., & Martinez, P. (2008). Land surface emissivity retrieval from different VNIR and TIR sensors. IEEE Transactions on Geoscience and Remote Sensing, 46 (2), 316–327.

Sekertekin, A., & Bonafoni, S. (2020a). Land Surface Temperature retrieval from Landsat 5, 7, and 8 over rural Areas: assessment of different retrieval algorithms and emissivity nodels and toolbox implementation. Remote Sensing 12 (2), 294. https://doi.org/10.3390/rs12020294.

Sekertekin, A., & Bonafoni S. (2020b). Sensitivity analysis and validation of daytime and nighttime Land Surface Temperature retrievals from Landsat 8 using different algorithms and emissivity Models. Remote Sensing 12 (17), 2776; https://doi.org/10.3390/rs12172776

Wang, F., Qin, Z., Song, C., Tu, L., Karnieli, A., & Zhao, S. (2015). An Improved Mono-Window Algorithm for Land Surface Temperature Retrieval from Landsat 8 Thermal Infrared Sensor Data. Remote Sensing 7, 4268–4289. https://doi.org/10.3390/rs70404268.

Windahl, E., Beurs, K. (2016). An intercomparison of Landsat land surface temperature retrieval methods under variable atmospheric conditions using in situ skin temperature. International Journal of Applied Earth Observation and Geoinformation, 51, 11–27, http://dx.doi.org/10.1016/j.jag.2016.04.003

Yu, X., Guo, X., & Wu, Z. (2014). Land Surface Temperature retrieval from Landsat 8 TIRS—comparison between Radiative Transfer Equation-Based method, Split Window Algorithm and Single Channel method. Remote Sensing, 6, 9829-9852; https://doi.org/10.3390/rs6109829.